Spin-resolved crossed Andreev reflection in ballistic heterostructures

Mikhail S. Kalenkov [a,b,1], Andrei D. Zaikin [a,b]

[a]*Forschungszentrum Karlsruhe, Institut für Nanotechnologie, 76021, Karlsruhe, Germany*
[b]*I.E. Tamm Department of Theoretical Physics, P.N. Lebedev Physics Institute, 119991 Moscow, Russia*

Abstract

We theoretically analyze non-local effects in electron transport across three-terminal ballistic normal-superconducting-normal (NSN) structures with spin-active interfaces. Subgap electrons entering S-electrode from one N-metal may form Cooper pairs with their counterparts penetrating from another N-metal. This phenomenon of crossed Andreev reflection is highly sensitive to electron spins and yields a rich variety of properties of non-local conductance which we describe non-perturbatively at arbitrary interface transmissions, voltages and temperatures. Our results can be applied to hybrid structures with normal, ferromagnetic and half-metallic electrodes and can be directly tested in future experiments.

Key words: Andreev reflection, proximity effect, hybrid structures, non-local conductance, spin-active interface
PACS: 74.45.+c, 73.23.-b, 74.78.Na

1. Introduction

Andreev reflection (AR) [1] is the main mechanism of low energy electron transport between a normal metal and a superconductor. This mechanism results in a number of interesting effects causing, e.g., a non-zero subgap conductance [2] of such hybrid structures. In systems with one superconducting (S) and several normal (N) terminals, e.g. NSN hybrid structures, electrons may suffer Andreev reflection at each of NS interfaces. Provided the distance between two NS interfaces L strongly exceeds the superconducting coherence length ξ, AR processes at these interfaces are independent. If, however, the distance L becomes comparable with ξ, two additional *non-local* processes should be taken into account (see Fig. 1). Firstly, an electron with subgap energy can directly penetrate from one N-metal into another through a superconductor. Since the subgap density of states in the superconductor

vanishes, the probability of this process should be suppressed by the factor $\sim \exp(-L/\xi)$. Secondly, an electron penetrating into the superconductor from the first N-terminal may form a Cooper pair together with another electron from the second N-terminal. In this case a hole goes into the second N-metal and AR becomes a non-local effect. The probability of this process – usually called crossed Andreev reflection (CAR) [3,4] – also decays as $\sim \exp(-L/\xi)$ and, in combination with direct electron transfer between normal electrodes, determines non-local conductance in hybrid multi-terminal structures. This non-local conductance can be directly measured in experiments and it has recently become a subject of intensive investigations.

Several experiments [5,6,7] allowed to clearly detect the non-local conductance in three-terminal NSN structures and demonstrated a rich variety of different features which unambiguous and detailed interpretation remains an important task for the future. At this point we note that in addition to CAR a number of other physical effects may consider-

---
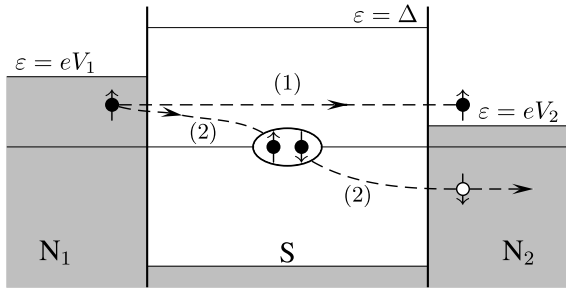
[1] Corresponding author. E-mail: kalenkov@lpi.ru

Fig. 1. Two elementary processes contributing to non-local conductance of an NSN device: (1) direct electron transfer and (2) crossed Andreev reflection.

Fig. 2. Schematics of our NSN device.

ably influence the observations. Among such effects we mention, e.g, charge imbalance (relevant close to the superconducting critical temperature [5,7]) and zero-bias anomalies in the Andreev conductance due to both disorder-enhanced interference of electrons [8,9,10] and Coulomb effects [10,11,12].

Theoretically CAR was analyzed within the perturbation theory in the transmission of NS interfaces in Refs. [13,14] where it was demonstrated that in the lowest order in the interface barrier transmission and at $T = 0$ CAR contribution to crossterminal conductance is exactly canceled by that from elastic electron cotunneling (indicated as (1) in Fig. 1), i.e. the non-local conductance turns out to vanish in this limit. Recently a non-trivial interplay between normal reflection, tunneling, local AR and CAR in three-terminal ballistic NSN devices was non-perturbatively analyzed to all orders in the interface transmissions [15]. This analysis allowed to determine an explicit dependence of the non-local conductance both on the transmissions of NS interfaces and on the length L, to set the maximum scale of the effect and to consider various important limits. The effect of disorder on CAR was recently studied in Refs. [16] (perturbatively in tunneling) and [17] (non-perturbatively in tunneling, for a device with normal terminals attached to a superconductor via an additional normal island). The interplay between CAR and Coulomb interaction effects was recently addressed in Refs. [18,19].

It is also important to mention that both AR and CAR should be sensitive to magnetic properties of normal electrodes because these processes essentially depend on spins of scattered electrons. First experiments on ferromagnet-superconductor-ferromagnet (FSF) structures [5] illustrated this point by demonstrating the dependence of non-local conductance on the polarization of ferromag-
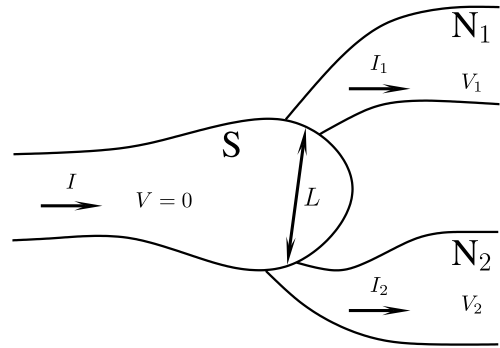
netic terminals. Hence, for better understanding of non-local effects in multiterminal hybrid proximity structures it is desirable to construct a theory of *spin-resolved* CAR. In the lowest order order in tunneling this task was accomplished in Ref. [13]. For FSF structures higher orders in the interface transmissions were considered in Refs. [20,21].

In this paper we are going to generalize our quasiclassical approach [15] and construct a theory of spin-resolved CAR to all orders in the interface transmissions. Instead of dealing directly with FSF devices we will consider NSN structures with spin-active interfaces. This model allows to distinguish spin-dependent contributions to the non-local conductance and to effectively mimic the situation of ferromagnetic and/or half-metallic electrodes.

The structure of the paper is as follows. In Sec. 2 we will introduce our model and discuss the quasiclassical formalism supplemented by the boundary conditions for Green-Keldysh functions which account for electron scattering at spin-active interfaces. Non-local electron transport in NSN structures with such interfaces will be analyzed in Sec. 3. Our main conclusions will be briefly summarized in Sec. 4. Technical details related to boundary conditions will be outlined in Appendix A.

2. The model and formalism

Let us consider three-terminal NSN structure depicted in Fig. 2. We will assume that all three metallic electrodes are non-magnetic and ballistic, i.e. the electron elastic mean free path in each metal is larger than any other relevant size scale. In order to resolve spin-dependent effects we will assume that both NS interfaces are spin-active, i.e. we will distinguish "spin-up" and "spin-down" transmissions of the first ($D_{1\uparrow}$ and $D_{1\downarrow}$) and the second ($D_{2\uparrow}$

and $D_{2\downarrow}$) SN interface. All these four transmissions may take any value from zero to one. The effective cross-sections of the two interfaces will be denoted respectively as $\mathcal{A}_1$ and $\mathcal{A}_2$. The distance between these interfaces L as well as other geometric parameters are assumed to be much larger than $\sqrt{\mathcal{A}_{1,2}}$, i.e. effectively both contacts are metallic constrictions. In this case the voltage drops only across SN interfaces and not inside large metallic electrodes. Hence, nonequilibrium (e.g. charge imbalance) effects related to the electric field penetration into the S-electrode can be neglected. In what follows we will also ignore Coulomb effects [10,11,12].

For convenience, we will set the electric potential of the S-electrode equal to zero, $V = 0$. In the presence of bias voltages V_1 and V_2 applied to two normal electrodes (see Fig. 2) the currents I_1 and I_2 will flow through SN_1 and SN_2 interfaces. These currents can be evaluated with the aid of the quasiclassical formalism of nonequilibrium Green-Eilenberger-Keldysh functions $\hat{g}^{R,A,K}$ [22] which we briefly specify below.

2.1. Quasiclassical equations

In the ballistic limit the corresponding equations take the form

$$\left[\varepsilon\hat{\tau}_3 + eV(\boldsymbol{r},t) - \hat{\Delta}(\boldsymbol{r},t), \hat{g}^{R,A,K}(\boldsymbol{p}_F,\varepsilon,\boldsymbol{r},t)\right] + \\ + i\boldsymbol{v}_F\nabla\hat{g}^{R,A,K}(\boldsymbol{p}_F,\varepsilon,\boldsymbol{r},t) = 0, \tag{1}$$

where $[\hat{a},\hat{b}] = \hat{a}\hat{b} - \hat{b}\hat{a}$, ε is the quasiparticle energy, $\boldsymbol{p}_F = m\boldsymbol{v}_F$ is the electron Fermi momentum vector and $\hat{\tau}_3$ is the Pauli matrix in Nambu space. The functions $\hat{g}^{R,A,K}$ also obey the normalization conditions $(\hat{g}^R)^2 = (\hat{g}^A)^2 = 1$ and $\hat{g}^R\hat{g}^K + \hat{g}^K\hat{g}^A = 0$. Here and below the product of matrices is defined as time convolution.

Green functions $\hat{g}^{R,A,K}$ and $\hat{\Delta}$ are 4×4 matrices in Nambu and spin spaces. In Nambu space they can be parameterized as

$$\hat{g}^{R,A,K} = \begin{pmatrix} g^{R,A,K} & f^{R,A,K} \\ \tilde{f}^{R,A,K} & \tilde{g}^{R,A,K} \end{pmatrix}, \quad \hat{\Delta} = \begin{pmatrix} 0 & \Delta i\sigma_2 \\ \Delta^* i\sigma_2 & 0 \end{pmatrix}, \tag{2}$$

where $g^{R,A,K}$, $f^{R,A,K}$, $\tilde{f}^{R,A,K}$, $\tilde{g}^{R,A,K}$ are 2×2 matrices in the spin space, Δ is the BCS order parameter and σ_i are Pauli matrices. For simplicity we will only consider the case of spin-singlet isotropic pairing in the superconducting electrode. The cur-

rent density is related to the Keldysh function $\hat{g}^K$ according to the standard formula

$$\boldsymbol{j}(\boldsymbol{r},t) = -\frac{eN_0}{8}\int d\varepsilon \left\langle \boldsymbol{v}_F\mathrm{Sp}[\hat{\tau}_3\hat{g}^K(\boldsymbol{p}_F,\varepsilon,\boldsymbol{r},t)]\right\rangle, \tag{3}$$

where $N_0 = mp_F/2\pi^2$ is the density of state at the Fermi level and angular brackets $\langle...\rangle$ denote averaging over the Fermi momentum.

2.2. Riccati parameterization

The above matrix Green-Keldysh functions can be conveniently parameterized by four Riccati amplitudes $\gamma^{R,A}$, $\tilde{\gamma}^{R,A}$ and two "distribution functions" x^K, $\tilde{x}^K$ (here we follow the notations adopted in Ref. [23]):

$$\hat{g}^K = 2\hat{N}^R \begin{pmatrix} x^K - \gamma^R\tilde{x}^K\tilde{\gamma}^A & -\gamma^R\tilde{x}^K + x^K\gamma^A \\ -\tilde{\gamma}^Rx^K + \tilde{x}^K\tilde{\gamma}^A & \tilde{x}^K - \tilde{\gamma}^Rx^K\gamma^A \end{pmatrix} \hat{N}^A, \tag{4}$$

where functions $\gamma^{R,A}$ and $\tilde{\gamma}^{R,A}$ are Riccati amplitudes

$$\hat{g}^{R,A} = \pm\hat{N}^{R,A}\begin{pmatrix} 1 + \gamma^{R,A}\tilde{\gamma}^{R,A} & 2\gamma^{R,A} \\ -2\tilde{\gamma}^{R,A} & -1 - \tilde{\gamma}^{R,A}\gamma^{R,A} \end{pmatrix}, \tag{5}$$

and $\hat{N}^{R,A}$ are the following matrices

$$\hat{N}^{R,A} = \begin{pmatrix} (1 - \gamma^{R,A}\tilde{\gamma}^{R,A})^{-1} & 0 \\ 0 & (1 - \tilde{\gamma}^{R,A}\gamma^{R,A})^{-1} \end{pmatrix}, \tag{6}$$

With the aid of the above parameterization one can identically transform the quasiclassical equations (1) into the following set of effectively decoupled equations for Riccati amplitudes and distribution functions [23]

$$i\boldsymbol{v}_F\nabla\gamma^{R,A} + [\varepsilon + eV(\boldsymbol{r},t)]\gamma^{R,A} + \gamma^{R,A}[\varepsilon - eV(\boldsymbol{r},t)] \\ = \gamma^{R,A}\Delta^*i\sigma_2\gamma^{R,A} - \Delta i\sigma_2, \tag{7}$$

$$i\boldsymbol{v}_F\nabla\tilde{\gamma}^{R,A} - [\varepsilon - eV(\boldsymbol{r},t)]\tilde{\gamma}^{R,A} - \tilde{\gamma}^{R,A}[\varepsilon + eV(\boldsymbol{r},t)] \\ = \tilde{\gamma}^{R,A}\Delta i\sigma_2\tilde{\gamma}^{R,A} - \Delta^*i\sigma_2, \tag{8}$$

$$i\boldsymbol{v}_F\nabla x^K + [\varepsilon + eV(\boldsymbol{r},t)]x^K - x^K[\varepsilon + eV(\boldsymbol{r},t)] \\ -\gamma^R\Delta^*i\sigma_2x^K - x^K\Delta i\sigma_2\tilde{\gamma}^A = 0, \tag{9}$$

$$i\boldsymbol{v}_F\nabla\tilde{x}^K - [\varepsilon - eV(\boldsymbol{r},t)]\tilde{x}^K + \tilde{x}^K[\varepsilon - eV(\boldsymbol{r},t)] \\ -\tilde{\gamma}^R\Delta i\sigma_2\tilde{x}^K - \tilde{x}^K\Delta^*i\sigma_2\gamma^A = 0. \tag{10}$$

3

S

N_1

N_2

$$1^{out} \qquad \tilde{\gamma}_{1'}^R, \Gamma_{1'}^R \quad \Gamma_1^R, \tilde{\Gamma}_1^A, X_1^K \qquad \tilde{\Gamma}_{1'}^R, \Gamma_{1'}^A, \tilde{X}_{1'}^K \qquad \Gamma_{2'}^R, \tilde{\Gamma}_{2'}^A, X_{2'}^K \qquad \tilde{\Gamma}_2^R, \Gamma_2^A, \tilde{X}_2^K \qquad 2^{in}$$
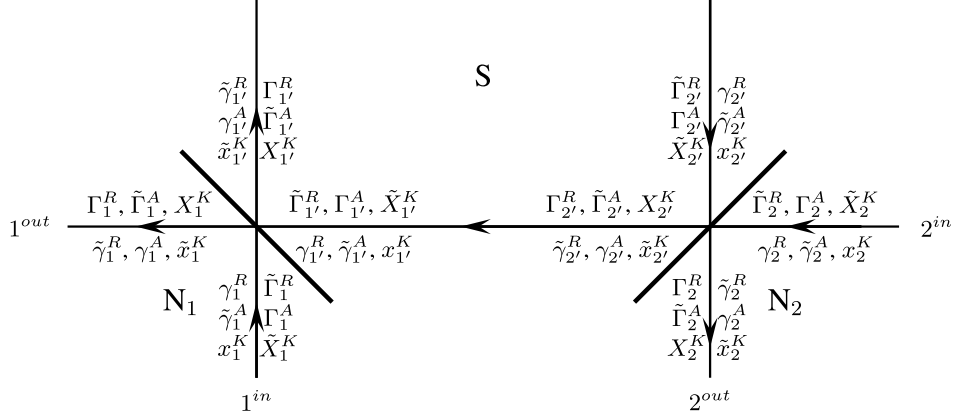
$$1^{in} \qquad\qquad 2^{out}$$

Fig. 3. Riccati amplitudes for incoming and outgoing trajectories for an NSN structure with two barriers. The arrows define quasiparticle momentum directions. We also indicate relevant Riccati amplitudes and distribution functions parameterizing the Green-Keldysh function for the corresponding trajectory.

Depending on the particular trajectory it is also convenient to introduce an additional "replica" of both Riccati amplitudes and distribution functions which – again following the notations adopted in Refs. [23,24]) will be denoted by capital letters Γ and X. These "capital" Riccati amplitudes and distribution functions obey the same (7)-(10) with the replacement $\gamma \to \Gamma$ and $x \to X$. The distinction between different Riccati amplitudes and distribution functions will be made explicit below.

2.3. Boundary conditions

Quasiclassical equations should be supplemented by appropriate boundary conditions at metallic interfaces. These conditions were initially formulated by Zaitsev [25] and later generalized to the case of spin-active (and specularly reflecting) interfaces in Ref. [28].

Before specifying these conditions we would like to note that the applicability of the above quasiclassical formalism with appropriate boundary conditions to hybrid structures with two (or more) barriers is, in general, a non-trivial issue [26,27] which requires a comment. Electrons scattered at different barriers may interfere and form bound states (resonances) which in general cannot be correctly described within the quasiclassical formalism employing Zaitsev boundary conditions. In our geometry, however, any relevant trajectory reaches each interface only once whereas the probability of multiple reflections at both interfaces is small in the parameter $\mathcal{A}_1 \mathcal{A}_2 / L^4 \ll 1$. Hence, resonances formed by multiply reflected electron waves can be neglected,

and our formalism remains adequate for the problem in question.

In what follows we will make use of boundary conditions formulated directly in terms of Riccati amplitudes and the distribution functions. In the case of spin-active interfaces these conditions are rather cumbersome [24] and therefore are relegated to Appendix.

In our three terminal geometry nonlocal conductance arises only from trajectories that cross both interfaces. Consider first the contribution of trajectories illustrated in Fig. 3 where, for simplicity, we assume identical polarizations of both interfaces SN_1 and SN_2. In this case the scattering matrix $\mathcal{S}$ for the first interface is defined in Eq. (A.23) while the $\mathcal{S}$-matrix for the second interface can be obtained from Eq. (A.23) by means of the replacement $1 \to 2$. Accordingly, all Riccati amplitudes have zero diagonal elements and all distribution functions have zero off-diagonal elements.

Finally, one needs to specify the asymptotic boundary conditions far from NS interfaces. Deep in metallic electrodes we have

$$\gamma_1^R = \tilde{\gamma}_1^R = \gamma_1^A = \tilde{\gamma}_1^A = 0, \qquad (11)$$

$$x_1^K = \tanh\left[\frac{\varepsilon + eV_1}{2T}\right], \quad \tilde{x}_1^K = -\tanh\left[\frac{\varepsilon - eV_1}{2T}\right], \qquad (12)$$

$$\gamma_2^R = \tilde{\gamma}_2^R = \gamma_2^A = \tilde{\gamma}_2^A = 0, \qquad (13)$$

$$x_2^K = \tanh\left[\frac{\varepsilon + eV_2}{2T}\right], \tilde{x}_2^K = -\tanh\left[\frac{\varepsilon - eV_2}{2T}\right], \qquad (14)$$

while in the bulk of superconducting electrode we have

4

$$\tilde{\gamma}_{1'}^R = -a(\varepsilon)i\sigma_2, \quad \gamma_{1'}^A = a^*(\varepsilon)i\sigma_2, \qquad (15)$$

$$\tilde{x}_{1'}^K = -[1 - |a(\varepsilon)|^2]\tanh\frac{\varepsilon}{2T}, \qquad (16)$$

$$\gamma_{2'}^R = a(\varepsilon)i\sigma_2, \quad \tilde{\gamma}_{2'}^A = -a^*(\varepsilon)i\sigma_2, \qquad (17)$$

$$x_{2'}^K = [1 - |a(\varepsilon)|^2]\tanh\frac{\varepsilon}{2T}, \qquad (18)$$

where $a(\varepsilon) = -(\varepsilon - \sqrt{\varepsilon^2 - \Delta^2})/\Delta$.

2.4. Green functions and non-local conductance

With the aid of the above equations and boundary conditions it is straightforward to evaluate the quasiclassical Green-Keldysh functions for our three-terminal device along whole trajectory. For instance, from the boundary conditions on the second interface we find

$$\Gamma_{2'}^R = \sqrt{R_{2\uparrow}R_{2\downarrow}}\begin{pmatrix} e^{i\theta_2} & 0 \\ 0 & e^{-i\theta_2} \end{pmatrix}i\sigma_2 a(\varepsilon). \qquad (19)$$

Then integrating equation (7) along trajectory connecting both interfaces and using Eq. (19) as the initial condition we arrive at the Riccati amplitude at the first interface:

$$\gamma_{1'}^R = \frac{\Gamma_{2'}^R + (\varepsilon\Gamma_{2'}^R + \Delta i\sigma_2)Q}{1 - (\varepsilon - \Delta\Gamma_{2'}^R i\sigma_2)Q},$$

$$Q = \frac{\tanh[i\Omega L/v_F]}{\Omega}, \quad \Omega = \sqrt{\varepsilon^2 - \Delta^2}. \qquad (20)$$

Similarly, integrating Eq. (9), one finds

$$x_{1'}^K = X_{2'}^K\frac{1 - \gamma_{1'}^R\tilde{\gamma}_{1'}^A}{1 - \Gamma_{2'}^R\tilde{\Gamma}_{2'}^A}. \qquad (21)$$

We also note that the relation $(\gamma^{R,A})^+ = \tilde{\Gamma}^{A,R}$ makes it unnecessary (while redundant) to separately calculate the amplitudes $\tilde{\gamma}_{1'}^A$ and $\tilde{\Gamma}_{2'}^A$.

Finally we arrive at the following general expression for the Green-Keldysh function g_1^K at SN_1 interface [15]

$$g_1^K = g_{11}^K(V_1) + \delta g_{12}^K(V_1) + \delta g_1^K(V_2), \qquad (22)$$

where the three different terms in the right-hand side correspond respectively to local contribution and two non-local corrections depending on V_1 and V_2. Since here we are only interested in the non-local conductance of our structure, it is sufficient to keep only the part of the Green-Keldysh function δg_1^K which depends on the voltage V_2 across the second interface. Combining the above results with the boundary conditions for the distribution functions

$X_{2'}^K$ and X_1^K at both interfaces respectively one immediately recovers δg_1^K. E.g., for the outgoing momenta directions (1^{out}) one gets

$$\delta g_1^{K(1)} = \delta X_1^K = 2(1 - \tanh^2 iL\Omega/v_F)$$
$$\times \begin{pmatrix} 1/P(\varepsilon, z_1, z_2) & 0 \\ 0 & 1/P(-\varepsilon, z_1, z_2) \end{pmatrix}$$
$$\times \left\{ \begin{pmatrix} D_{1\uparrow}D_{2\uparrow} & 0 \\ 0 & D_{1\downarrow}D_{2\downarrow} \end{pmatrix}\tanh\frac{\varepsilon + eV_2}{2T} \right.$$
$$\left. + |a|^2\begin{pmatrix} D_{1\uparrow}D_{2\downarrow}R_{2\uparrow} & 0 \\ 0 & D_{1\downarrow}D_{2\uparrow}R_{2\downarrow} \end{pmatrix}\tanh\frac{\varepsilon - eV_2}{2T} \right\}, \tag{23}$$

where δX_1^K is the V_2-dependent part of the X_1^K distribution function, $z_i = \sqrt{R_{i\uparrow}R_{i\downarrow}}\exp(i\theta_i)$, $i = 1, 2$ $R_{i\uparrow(\downarrow)}$ are the spin-sensitive reflection coefficients, θ_i are the spin-mixing angles and

$$P(\varepsilon, z_1, z_2) = \left| 1 - z_1z_2a^2 - \frac{\tanh iL\Omega/v_F}{\Omega} \right.$$
$$\left. \times \left[\varepsilon(1 + z_1z_2a^2) + a\Delta(z_1 + z_2)\right] \right|^2. \quad (24)$$

Reversing momenta directions for all trajectories in Fig. 3 yields the second set of trajectories which also contributes to the non-local conductance. The corresponding expression for the V_2-dependent part of the Green-Keldysh function $\delta g_1^{K(2)}$ at the normal metal side of the first interface is derived analogously to Eq. (23). Again for the outgoing momenta directions we obtain

$$\delta g_1^{K(2)} = 2(1 - \tanh^2 iL\Omega/v_F)$$
$$\times \begin{pmatrix} 1/P(\varepsilon, z_1, z_2) & 0 \\ 0 & 1/P(-\varepsilon, z_1, z_2) \end{pmatrix}$$
$$\times \left\{ |a|^4\begin{pmatrix} D_{1\uparrow}R_{1\downarrow}D_{2\uparrow}R_{2\downarrow} & 0 \\ 0 & D_{1\downarrow}R_{1\uparrow}D_{2\downarrow}R_{2\uparrow} \end{pmatrix}\tanh\frac{\varepsilon + eV_2}{2T} \right.$$
$$\left. + |a|^2\begin{pmatrix} D_{1\uparrow}R_{1\downarrow}D_{2\downarrow} & 0 \\ 0 & D_{1\downarrow}R_{1\uparrow}D_{2\uparrow} \end{pmatrix}\tanh\frac{\varepsilon - eV_2}{2T} \right\}. \tag{25}$$

Finally we note that in the expression for function g^K there also exist terms corresponding to incoming momenta directions (again on the normal metal side of the first interface). However, those terms do not

depend on the voltage V_2 and, hence, do not contribute to the non-local conductance at all. Thus, Eqs. (23) and (25) already contain complete information which allows to evaluate the non-local current across the first interface. This task will be accomplished below.

3. Nonlocal conductance

3.1. General results

With the aid of general expressions for the Green-Keldysh functions obtained here it is possible to demonstrate that the total currents across the first and the second interface NS interfaces I_1 and I_2 have the form [15]

$$I_1 = I_{11}(V_1) + I_{12}(V_2), \qquad (26)$$
$$I_2 = I_{21}(V_1) + I_{22}(V_2). \qquad (27)$$

Here we are interested in the non-local part of the current $I_{12}(V_2)$ across the first interface. Substituting (23) and (25) into (3) we obtain

$$I_{12}(V_2) = -\frac{G_0}{4e} \int d\varepsilon \left[\tanh\frac{\varepsilon + eV_2}{2T} - \tanh\frac{\varepsilon}{2T} \right]$$
$$\times (1 - \tanh^2 iL\Omega/v_F)$$
$$\times \left(\frac{D_{1\uparrow}D_{2\uparrow}[1 + |a|^4 R_{1\downarrow}R_{2\downarrow}] - |a|^2(D_{1\downarrow}D_{2\uparrow}[R_{2\downarrow} + R_{1\uparrow}]}{P(\varepsilon, z_1, z_2)} \right.$$
$$\left. + \frac{D_{1\downarrow}D_{2\downarrow}[1 + |a|^4 R_{1\uparrow}R_{2\uparrow}] - |a|^2(D_{1\uparrow}D_{2\downarrow}[R_{2\uparrow} + R_{1\downarrow}]}{P(-\varepsilon, z_1, z_2)} \right)$$
$$(28)$$

where

$$G_{N_{12}} = G_0 \frac{D_{1\uparrow}D_{2\uparrow} + D_{1\downarrow}D_{2\downarrow}}{2} \qquad (29)$$

is the non-local conductance of our device in the normal state,

$$G_0 = \frac{8\gamma_1\gamma_2 \mathcal{N}_1 \mathcal{N}_2}{R_q p_F^2 L^2},$$

$p_F\gamma_{1(2)}$ is normal to the first (second) interface component of the Fermi momentum for electrons propagating straight between the interfaces, $\mathcal{N}_{1,2} = p_F^2 \mathcal{A}_{1,2}/4\pi$ define the number of conducting channels of the corresponding interface, $R_q = 2\pi/e^2$ is the quantum resistance unit.

Eq. (28) is the central result of our paper. It fully determines the non-local spin-dependent current in our three-terminal ballistic NSN structure at arbitrary interface transmissions, voltages and temperature. It is also convenient to introduce the non-local differential conductance $G_{12}(V_2) = -\partial I_{12}/\partial V_2$. In

the limit $T, V_{1,2} \ll \Delta$ only subgap quasiparticles contribute to the current and the differential conductance becomes voltage-independent. We have $I_{12} = -G_{12}V_2$, where

$$G_{12} = G_0(1 - \tanh^2 L\Delta/v_F)$$
$$\times \frac{(D_{1\uparrow} - D_{1\downarrow})(D_{2\uparrow} - D_{2\downarrow}) + D_{1\uparrow}D_{1\downarrow}D_{2\uparrow}D_{2\downarrow}}{P(0, z_1, z_2)}.$$
$$(30)$$

For spin-isotropic interfaces Eqs. (30) and (28) yield the results obtained previously in [15]. In the lowest (first order) order in the transmissions of both interfaces Eq. (30) reduces to the result by Falci *et al.* [13] provided we assume that the ratio $D_{1(2)\uparrow}/D_{1(2)\downarrow}$ coincides with that of spin-up and spin-down densities of states in the first (second) ferromagnetic electrode. We also note that, provided at least one of the interfaces is spin-isotropic, the conductance (30) is proportional to the product of all four transmissions $D_{1\uparrow}D_{1\downarrow}D_{2\uparrow}D_{2\downarrow}$, i.e. it differs from zero only due to processes involving scattering with both spin projections in both normal electrodes.

As in the case of spin-isotropic interfaces the value G_{12} (30) gets strongly suppressed with increasing L, and this dependence on L is in general non-exponential reducing to $G_{12} \propto \exp(-2L\Delta/v_F)$ either in the limit of small transmissions or large $L \gg v_F/\Delta$.

In the spin-degenerate case for a given L the non-local conductance reaches its maximum reflectionless barriers $D_{1,2} = 1$. Interestingly, in this case for small $L \ll v_F/\Delta$ the conductance G_{12} identically coincides with its normal state value $G_{N_{12}}$ at any temperature and voltage. For $L \to 0$ there is "no space" for CAR to develop on these trajectories and, hence, CAR contribution to G_{12} vanishes, whereas direct transfer of electrons between N$_1$ and N$_2$ remains unaffected by superconductivity in this limit.

The situation changes provided at least one of the transmissions is smaller than one. In this case scattering at SN interfaces mixes up trajectories connecting N$_1$ and N$_2$ terminals with ones going deep into and coming from the superconductor. As a result, CAR contribution to G_{12} does not vanish even in the limit $L \to 0$ and G_{12} turns out to be smaller than $G_{N_{12}}$.

3.2. Polarized interfaces

Let us now turn to the limit of highly polarized interfaces which is accounted for by either spin-up
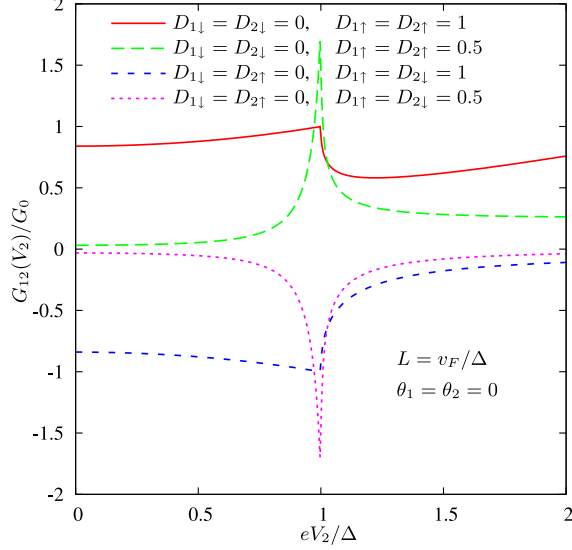
Fig. 4. Zero temperature differential non-local conductance as a function of voltage for a half-metal/superconductor/half-metal structure. Different curves correspond to different interface transmissions and different orientations of the half-metal magnetizations.

or spin-down transmission of each interface going to zero. In this limit our model describes an HSH structure, where H stands for fully spin-polarized half-metallic electrodes. In the case of parallel magnetization of both half-metals ($D_{1\uparrow} = D_1$, $D_{1\downarrow} = 0$, $D_{2\uparrow} = D_2$, and $D_{2\downarrow} = 0$) we obtain

$$I_{12}^{\uparrow\uparrow}(V_2) = -\frac{G_0}{4e} \int d\varepsilon \left[\tanh \frac{\varepsilon + eV_2}{2T} - \tanh \frac{\varepsilon}{2T} \right]$$
$$\times (1 - \tanh^2 iL\Omega/v_F) \frac{D_1 D_2 (1 + |a|^4)}{P(\varepsilon, z_1, z_2)}, \quad (31)$$

while in the case of antiparallel magnetization ($D_{1\uparrow} = D_1$, $D_{1\downarrow} = 0$, $D_{2\uparrow} = 0$, and $D_{2\downarrow} = D_2$) we find

$$I_{12}^{\uparrow\downarrow}(V_2) = +\frac{G_0}{4e} \int d\varepsilon \left[\tanh \frac{\varepsilon + eV_2}{2T} - \tanh \frac{\varepsilon}{2T} \right]$$
$$\times (1 - \tanh^2 iL\Omega/v_F) \frac{D_1 D_2 2|a|^2}{P(-\varepsilon, z_1, z_2)}, \quad (32)$$

i.e. the non-local conductances (31) and (32) have opposite signs. Some typical curves for the differential non-local conductance are presented in Fig. 4 at sufficiently high interface transmissions and zero spin mixing angles. With decreasing interface transmissions low voltage non-local conductance diminishes and sharp peaks at voltages $eV_2 = \pm\Delta$ appear.

We will now turn to asymmetric HSN heterostructures with one half-metallic and one spin-isotropic electrode. In this case the non-local cur-
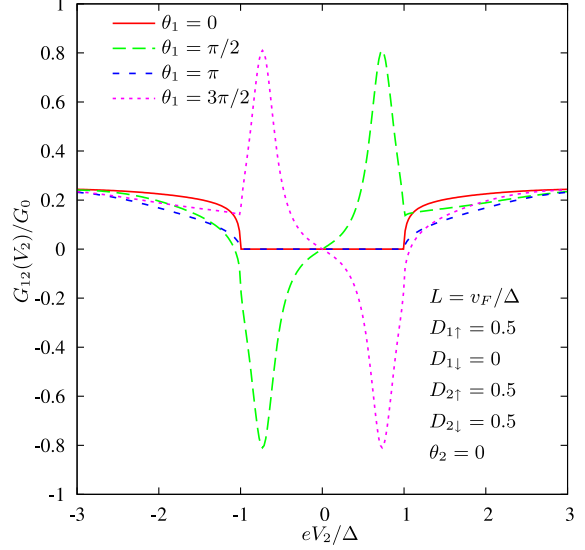

Fig. 5. Zero temperature differential non-local conductance as a function of voltage for a half-metal/superconductor/metal structure. Different curves correspond to different values of the spin-mixing angle θ_1.

rent does not depend on the magnetization direction of the half-metal. Below we will distinguish NSH and HSN configurations. In the case of metal/superconductor/half-metal (NSH) structures ($D_{1\uparrow} = D_{1\downarrow} = D_1$, $D_{2\uparrow} = D_2$, $D_{2\downarrow} = 0$) we obtain

$$I_{12}(V_2) = -\frac{G_0}{4e} \int d\varepsilon \left[\tanh \frac{\varepsilon + eV_2}{2T} - \tanh \frac{\varepsilon}{2T} \right]$$
$$\times (1 - \tanh^2 iL\Omega/v_F) \frac{D_1 D_2 (1 - |a|^2)(1 - R_1|a|^2)}{P(\varepsilon, z_1, z_2)}. \quad (33)$$

We note that in this case the spectral current is identically zero at all subgap energies $|\varepsilon| < \Delta$. The sign of the non-local current and differential conductance remain the same as in the normal state. In the reversed situation of a half-metal/superconductor/metal (HSN) structure ($D_{1\uparrow} = D_1$, $D_{1\downarrow} = 0$, $D_{2\uparrow} = D_{2\downarrow} = D_2$) our general results yield

$$I_{12}(V_2) = -\frac{G_0}{4e} \int d\varepsilon \left[\tanh \frac{\varepsilon + eV_2}{2T} - \tanh \frac{\varepsilon}{2T} \right]$$
$$\times D_1 D_2 (1 - \tanh^2 iL\Omega/v_F)$$
$$\times \left(\frac{1 + |a|^4 R_2}{P(\varepsilon, z_1, z_2)} - \frac{|a|^2 (1 + R_2)}{P(-\varepsilon, z_1, z_2)} \right). \quad (34)$$

In contrast to Eq. (33), here the spectral current does not vanish at subgap energies provided the spin-mixing angle θ_1 differs from zero. The sign of the non-local conductance in this geometry depends
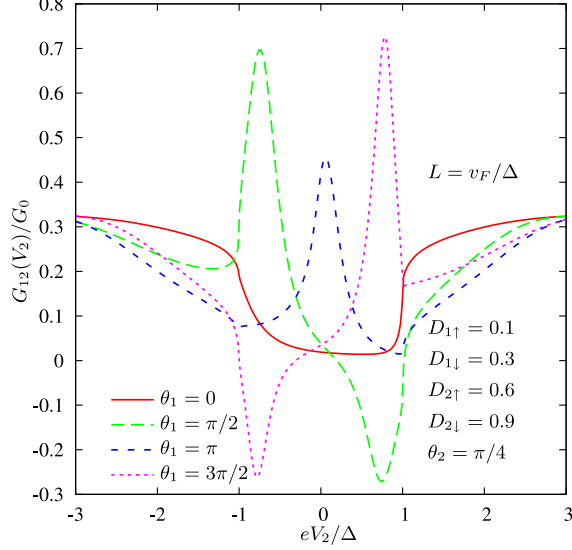
Fig. 6. Zero temperature differential non-local conductance as a function of voltage for a general case of an NSN structure with non-zero transmissions $D_{1\uparrow}$, $D_{1\downarrow}$, $D_{2\uparrow}$ and $D_{2\downarrow}$ and non-zero spin-mixing angles θ_1 and θ_2.

on both applied voltage V_2 and spin-mixing angle θ_1. The zero temperature non-local conductance evaluated with the aid of Eq. (34) at sufficiently high interface transmissions and different spin-mixing angles is depicted in Fig. 5.

In general, the voltage dependence of the non-local current is very sensitive to the interface transmissions and – in particular – to values of spin-mixing angles $\theta_{1,2}$. Typical curves illustrating the voltage dependence of the differential non-local conductance are shown in Fig. 6 at different spin-mixing angles. Positions of the peaks correspond to energies of the quasibound states in NSN structures.

4. Conclusions

In this paper we have developed a non-perturbative theory of spin-resolved non-local electron transport in ballistic NSN three-terminal structures with spin-active interfaces. Our theory applies at arbitrary interface transmissions and allows to fully describe a non-trivial interplay between spin-sensitive normal scattering, local and non-local Andreev reflection at SN interfaces. We have evaluated the non-local conductance of our NSN device at arbitrary voltages and temperatures and observed a number of interesting properties of such structures with spin-active interfaces. Our results can be applied to various NSN hybrid structures, including systems with fer-
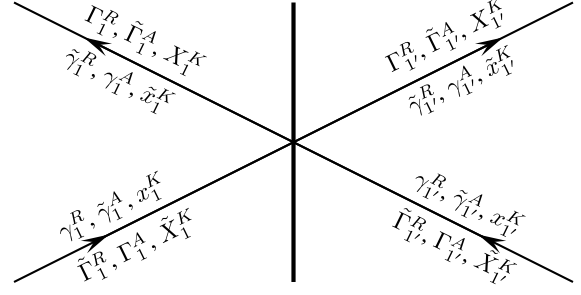

Fig. A.1. Riccati amplitudes for incoming and outgoing trajectories from the both sides of the interface.

romagnetic and half-metallic electrodes, and can be directly tested in future experiments.

Appendix A. Boundary conditions for spin-active interfaces

Let us explicitly specify the relations between Riccati amplitudes and distribution functions for incoming and outgoing trajectories at the first interface, see Fig. A.1. The boundary conditions for Γ_1^R, $\tilde{\Gamma}_1^A$ and X_1^K can be written in the form [24]

$$\Gamma_1^R = r_{1l}^R \gamma_1^R \underline{S}_{11}^+ + t_{1l}^R \gamma_{1'}^R \underline{S}_{11'}^+, \qquad (A.1)$$

$$\tilde{\Gamma}_1^A = \underline{S}_{11} \tilde{\gamma}_1^A \tilde{r}_{1r}^A + \underline{S}_{11'} \tilde{\gamma}_1^A \tilde{t}_{1r}^A, \qquad (A.2)$$

$$X_1^K = r_{1l}^R x_1^K \tilde{r}_{1r}^A + t_{1l}^R x_{1'}^K \tilde{t}_{1r}^A - a_{1l}^R \tilde{x}_{1'}^K \tilde{a}_{1r}^A. \qquad (A.3)$$

Here the transmission (t), reflection (r), and branch-conversion (a) amplitudes are defined as follows:

$$r_{1l}^R = +[(\beta_{1'1}^R)^{-1} S_{11}^+ - (\beta_{1'1'}^R)^{-1} S_{11'}^+]^{-1} (\beta_{1'1}^R)^{-1},$$
$$(A.4)$$

$$t_{1l}^R = -[(\beta_{1'1}^R)^{-1} S_{11}^+ - (\beta_{1'1'}^R)^{-1} S_{11'}^+]^{-1} (\beta_{1'1'}^R)^{-1},$$
$$(A.5)$$

$$\tilde{r}_{1r}^A = +(\beta_{1'1}^A)^{-1}[S_{11}(\beta_{1'1}^A)^{-1} - S_{11'}(\beta_{1'1'}^A)^{-1}]^{-1},$$
$$(A.6)$$

$$\tilde{t}_{1r}^A = -(\beta_{1'1'}^A)^{-1}[S_{11}(\beta_{1'1}^A)^{-1} - S_{11'}(\beta_{1'1'}^A)^{-1}]^{-1},$$
$$(A.7)$$

$$a_{1l}^R = (\Gamma_1^R \underline{S}_{11} - S_{11} \gamma_1^R)(\tilde{\beta}_{1'1'}^R)^{-1}, \qquad (A.8)$$

$$\tilde{a}_{1r}^A = (\tilde{\beta}_{11'}^A)^{-1}(\underline{S}_{11}^+ \tilde{\Gamma}_1^A - \tilde{\gamma}_1^A S_{11}^+), \qquad (A.9)$$

where

$$\beta_{ij}^R = S_{ij}^+ - \gamma_j^R \underline{S}_{ij}^+ \tilde{\gamma}_i^R, \quad \tilde{\beta}_{ij}^R = \underline{S}_{ji} - \tilde{\gamma}_j^R S_{ji} \gamma_i^R,$$
$$(A.10)$$

$$\beta_{ij}^A = S_{ij} - \gamma_i^A \underline{S}_{ij} \tilde{\gamma}_j^A, \quad \tilde{\beta}_{ij}^A = \underline{S}_{ji}^+ - \tilde{\gamma}_i^A S_{ji}^+ \gamma_j^A.$$
$$(A.11)$$

Similarly, the boundary conditions for $\tilde{\Gamma}_1^R$, Γ_1^A, and $\tilde{X}_1^K$ are:

$$\tilde{\Gamma}_1^R = \tilde{r}_{1l}^R \tilde{\gamma}_1^R S_{11} + \tilde{t}_{1l}^R \tilde{\gamma}_{1'}^R S_{1'1}, \qquad (A.12)$$

$$\Gamma_1^A = S_{11}^+ \gamma_1^A r_{1r}^A + S_{1'1}^+ \gamma_{1'}^A t_{1r}^A, \qquad (A.13)$$

$$\tilde{X}_1^K = \tilde{r}_{1l}^R \tilde{x}_1^K r_{1r}^A + \tilde{t}_{1l}^R \tilde{x}_{1'}^K t_{1r}^A - \tilde{a}_{1l}^R x_{1'}^K a_{1r}^A, \quad (A.14)$$

where

$$\tilde{r}_{1l}^R = +[(\tilde{\beta}_{1'1}^R)^{-1}\underline{S}_{11} - (\tilde{\beta}_{1'1'}^R)^{-1}\underline{S}_{1'1}]^{-1}(\tilde{\beta}_{1'1}^R)^{-1}, \qquad (A.15)$$

$$t_{1l}^R = -[(\tilde{\beta}_{1'1}^R)^{-1}\underline{S}_{11} - (\tilde{\beta}_{1'1'}^R)^{-1}\underline{S}_{1'1}]^{-1}(\tilde{\beta}_{1'1'}^R)^{-1}, \qquad (A.16)$$

$$r_{1r}^A = +(\tilde{\beta}_{1'1}^A)^{-1}[\underline{S}_{11}^+(\tilde{\beta}_{1'1}^A)^{-1} - \underline{S}_{1'1}^+(\tilde{\beta}_{1'1'}^A)^{-1}]^{-1}, \qquad (A.17)$$

$$\tilde{t}_{1r}^A = -(\tilde{\beta}_{1'1'}^A)^{-1}[\underline{S}_{11}^+(\tilde{\beta}_{1'1}^A)^{-1} - \underline{S}_{1'1}^+(\tilde{\beta}_{1'1'}^A)^{-1}]^{-1}, \qquad (A.18)$$

$$a_{1l}^R = (\Gamma_1^R \underline{S}_{11} - S_{11}\gamma_1^R)(\tilde{\beta}_{11'}^R)^{-1}, \qquad (A.19)$$

$$\tilde{a}_{1r}^A = (\tilde{\beta}_{11'}^A)^{-1}(\underline{S}_{11}^+ \tilde{\Gamma}_1^A - \tilde{\gamma}_1^A S_{11}^+). \qquad (A.20)$$

Boundary conditions for $\Gamma_{1'}^{R,A}$, $\tilde{\Gamma}_{1'}^{R,A}$, $X_{1'}^K$ and $\tilde{X}_{1'}^K$ can be obtained from the above equations by means of the replacement $1 \leftrightarrow 1'$.

Matrices S_{11}, $S_{11'}$, $S_{1'1}$, and $S_{1'1'}$ are the components of the $\mathcal{S}$-matrix describing electron scattering at the first interface:

$$\mathcal{S} = \begin{pmatrix} S_{11} & S_{11'} \\ S_{1'1} & S_{1'1'} \end{pmatrix}, \quad \mathcal{S}\mathcal{S}^+ = 1 \qquad (A.21)$$

For specularly reflecting interfaces with inversion symmetry elements of the $\mathcal{S}$-matrix have the following form

$$S_{11} = S_{1'1'} = \begin{pmatrix} \sqrt{R_{1\uparrow}}e^{i\theta_1/2} & 0 \\ 0 & \sqrt{R_{1\downarrow}}e^{-i\theta_1/2} \end{pmatrix}, \qquad (A.22)$$

$$S_{11'} = S_{11'} = i\begin{pmatrix} \sqrt{D_{1\uparrow}}e^{i\theta_1/2} & 0 \\ 0 & \sqrt{D_{1\downarrow}}e^{-i\theta_1/2} \end{pmatrix}, \qquad (A.23)$$

where $D_{1\uparrow}$ and $D_{1\downarrow}$ are interface transmission for spin-up and spin-down electron. The spin-mixing angle θ_1 accounts for the difference between scattering phases for processes with opposite spin directions. The condition $\underline{S}_{ij} = S_{ij}$ holds provided there exists reflection symmetry in the plane perpendicular to the interface.

[1] A.F. Andreev, Zh. Eksp. Teor. Fiz. 46 (1964)1823 [Sov. Phys. JETP 19 (1964) 1228].
[2] G.E. Blonder, M. Tinkham, T.M. Klapwijk, Phys. Rev. B 25 (1982) 4515.
[3] J.M. Byers, M.E. Flatte, Phys. Rev. Lett. 74 (1995) 306.
[4] G. Deutscher, D. Feinberg, Appl. Phys. Lett. 76 (2000) 487.
[5] D. Beckmann, H.B. Weber, H. v. Löhneysen, Phys. Rev. Lett. 93 (2004) 197003; D. Beckmann, H. v. Löhneysen, cond-mat/0609766.
[6] S. Russo, M. Kroug, T.M. Klapwijk, A.F. Morpurgo, Phys. Rev. Lett. 95 (2005) 027002.
[7] P. Cadden-Zimansky, V. Chandrasekhar, Phys. Rev. Lett. 97 (2006) 237003.
[8] A.F. Volkov, A.V. Zaitsev, T.M. Klapwijk, Physica C 210 (1993) 21.
[9] F.W.J. Hekking, Yu.V. Nazarov, Phys. Rev. Lett. 71 (1993) 1625.
[10] A.D. Zaikin, Phyica B 203 (1994) 255.
[11] A. Huck, F.W.J. Hekking, B. Kramer, Europhys. Lett. 41 (1998) 201.
[12] A.V. Galaktionov, A.D. Zaikin, Phys. Rev. B 73 (2006) 184522.
[13] G. Falci, D. Feinberg, F.W.J. Hekking, Europhys. Lett. 54 (2001) 255.
[14] G. Bignon, M. Houset, F. Pistolesi, F.W.J. Hekking, Europhys. Lett. 67 (2004) 110.
[15] M.S. Kalenkov, A.D. Zaikin, Phys. Rev. B 75 (2007) 172503. .
[16] A. Brinkman, A.A. Golubov, Phys. Rev. B 74 (2006) 214512.
[17] J.P. Morten, A. Brataas, W. Belzig, Phys. Rev. B 74 (2006) 214510.
[18] A. Levy Yeyati, F.S. Bergeret, A. Martin-Rodero, T.M. Klapwijk, cond-mat/0612027.
[19] D.S. Golubev, A.D. Zaikin, in preparation.
[20] R. Melin, D. Feinberg, Phys. Rev. B 70 (2004) 174509.
[21] R. Melin, Phys. Rev. B 73 (2006) 174512.
[22] For a review see, e.g., W. Belzig, F. Wilhelm, C. Bruder, G. Schön, A.D. Zaikin, Superlatt. Microstruct. 25 (1999) 1251.
[23] M. Eschrig, Phys. Rev. B 61 (2000) 9061.
[24] E. Zhao, T. Löfwander, J.A. Sauls, Phys. Rev. B 70 (2004) 134501.
[25] A.V. Zaitsev, Sov. Phys. JETP 59 (1984) 1015.
[26] A.V. Galaktionov, A.D. Zaikin, Phys. Rev. B 65 (2002) 184507.
[27] M. Ozana, A. Shelankov, Phys. Rev. B 65 (2002) 014510.
[28] A. Millis, D. Rainer, J.A. Sauls, Phys. Rev. B 38 (1988) 4504.

References